Morphology-Controlled Synthesis of $WO_{2.72}$ Nanostructures and Their photocatalytic Properties

Table of contents

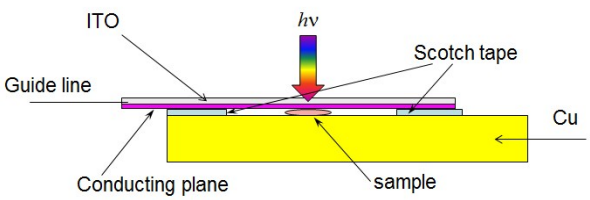

Figure S 1 Schematic of sample loading method for the SPC measurement.

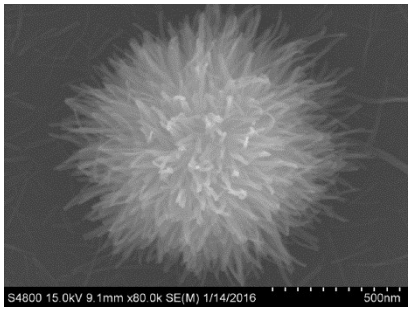

Figure S 2 SEM image of the urchin-like $WO_{2.72}$ nanostructure.

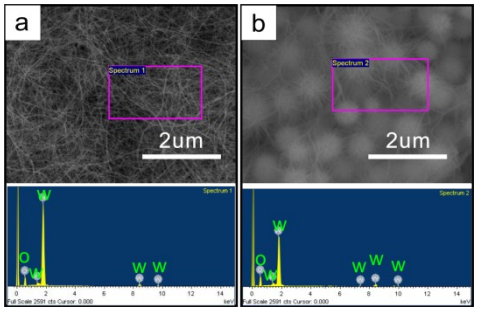

Figure S 3 EDS spectra of the $WO_{2.72}$ nanowires (a) and the urchin-like $WO_{2.72}$ nanostructures (b).

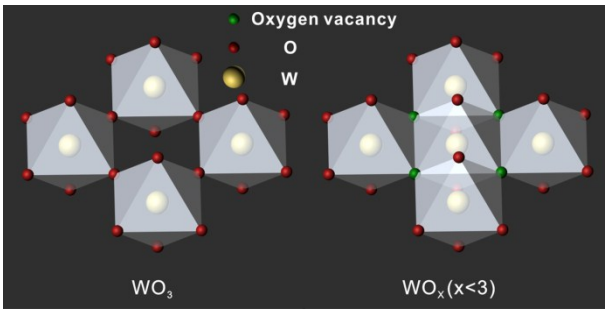

Figure S 4 Structure illustration of WO_3（WO_6 units were connected by co-corner, left） and WO_X(x<3). (WO_6 units were connected partially by co-edge, right).

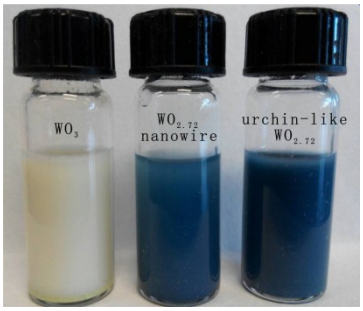

Figure S 5 Color conversion of the samples.

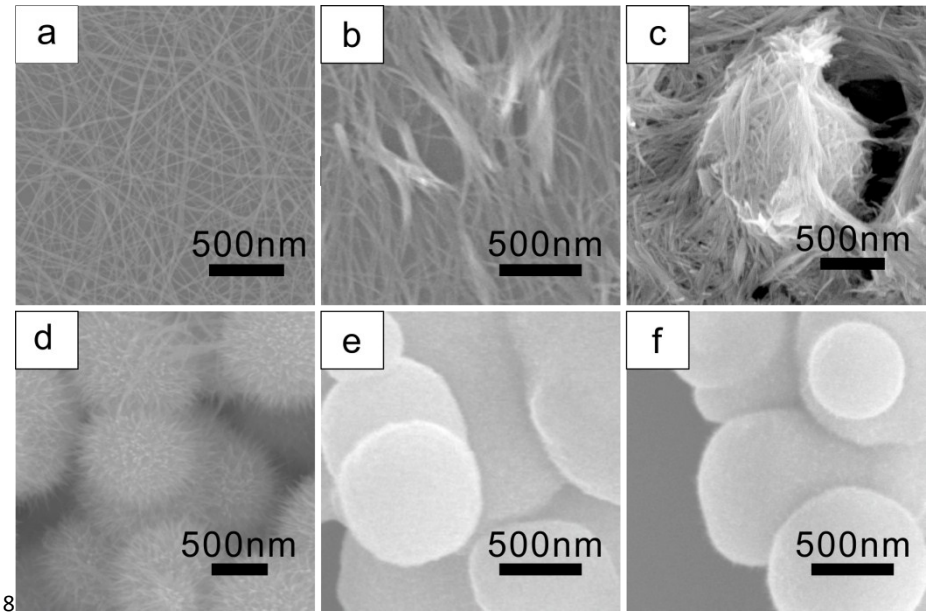

Figure S 6 SEM images of $WO_{2.72}$ nanostructures obtained by treating at 180°C for 10 h with C_{WCl6}=0.5g/L (a), C_{WCl6}=1g/L (b), C_{WCl6}=3g/L (c) C_{WCl6}=5g/L (d) C_{WCl6}=7g/L (e) and C_{WCl6}=10g/L (f).

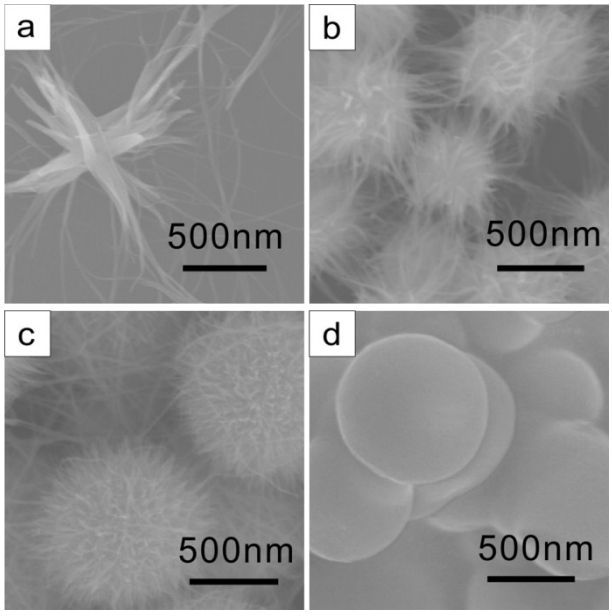

Figure S 7 SEM images of urchin-like $WO_{2.72}$ nanostructures obtained by reacting for 3h(a)，6h(b)，10h(c) and 24h(d);(C_{WCl6}=5g/L, 180°C).

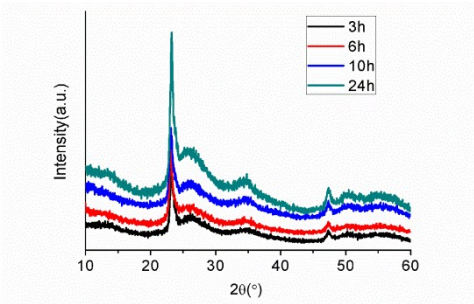

Figure S 8 XRD patterns of WCl_6 solvothermal treated in different times.

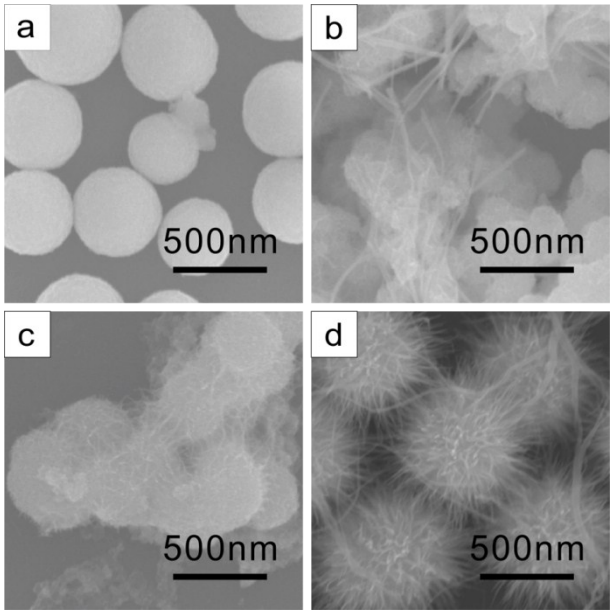

Figure S 9 SEM images of $WO_{2.72}$ nanostructures which were obtained at 120 °C (a), 140 °C (b), 160 °C (c) and 180 °C (d) respectively ;(C_{WCl6}=5g/L, 10h).

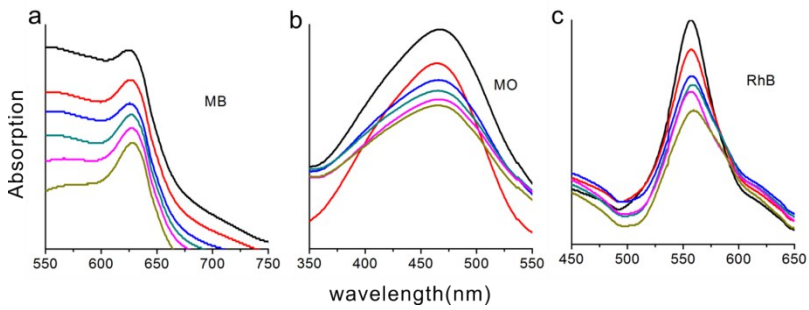

Figure S 10 Changing UV-Vis spectra of MB (a), and MO (b) Rh B (c) aqueous solution in the presence of $WO_{2.72}$ nanowires under UV light irradiation.

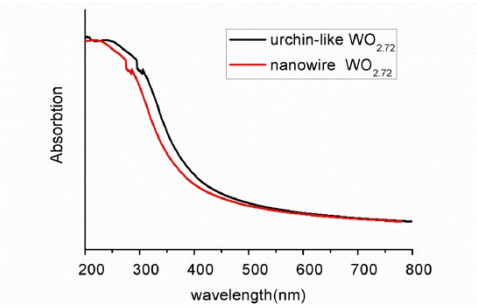

Figure S 11 UV/Vis absorption spectra of the $WO_{2.72}$ nanowires (red) and urchin-like $WO_{2.72}$ nanostructures (black) after photocatalysis.

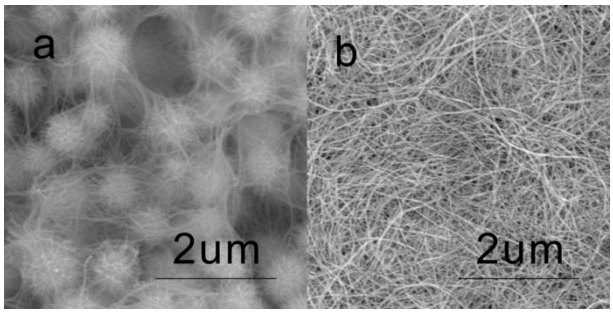

Figure S 12 SEM images of the urchin-like $WO_{2.72}$ nanostructures (a) and $WO_{2.72}$ nanowires (b) after photocatalysis.

Table S 1 BET surface areas of WO2.72 nanowires, urchin-like WO2.72 nanostructures and commercial ones.

material	$WO_{2.72}$ nanowires	Urchin-like $WO_{2.72}$ nanosructures	Commercial ones
BET(m^2/g)	189.3	177.9	11.7